Photografting Polymerization of Polyacrylamide on Poly(3-hydroxybutyrate-*co*-3-hydroxyvalerate) Films. II. Wettability and Crystallization Behaviors of Poly(3-hydroxybutyrate-*co*-3-hydroxyvalerate)-*graft*-Polyacrylamide Films

Yingjun Wang,[1,2] Yu Ke,[1] Li Ren,[1,2] Gang Wu,[1,2] Xiaofeng Chen[1,2]

[1]*Biomaterial Research Institute, College of Material Science and Engineering, South China University of Technology, Guangzhou, China*
[2]*Key Laboratory of Specially Functional Material and Advanced Manufacturing Technology, South China University of Technology, Guangzhou, China*

Received 22 May 2007; accepted 16 September 2007
DOI 10.1002/app.27415
Published online 6 December 2007 in Wiley InterScience (www.interscience.wiley.com).

ABSTRACT: The wettability and crystallization behaviors of poly(3-hydroxybutyrate-*co*-3-hydroxyvalerate) (PHBV)-*graft*-polyacrylamide (PAM) films were studied. X-ray photoelectron spectroscopy analyses illustrated that about 62 atom % of the total polar functionalities on the grafted film with 17% grafting percentage (GP) was amide groups. Wide-angle X-ray diffraction results suggest that grafted PAM induced defects in PHBV crystals and influenced their crystal structure. Differential scanning calorimetry (DSC) spectra showed the two melting regions, 60–90 and 145–170°C, of the imperfect PHBV crystals of the grafted films. Grafted PAM could suppress the recrystallization of PHBV, which was consistent with the polarizing optical microscopy results, in which the maximum PHBV spherulite diameter decreased from 350 μm for the PHBV film to 50 μm for the film with 53% GP. In addition, DSC studies revealed that the crystallinity of the grafted films decreased with increasing GP, which facilitated the diffusion of water into the films. The water contact angle of grafted films decreased and the water-swelling percentage increased as GP went up. These results demonstrate the potential of PHBV-*g*-PAM for wettable surface constructs in tissue engineering applications. © 2007 Wiley Periodicals, Inc. J Appl Polym Sci 107: 3765–3772, 2008

Key words: crystallization; hydrophilic polymers; films; PHBV; photopolymerization

INTRODUCTION

Tissue engineering, which is used to restore, maintain, or enhance tissues and organs, has drawn great attention in recent years.[1] Tissue engineering scaffolds are designed to provide a support structure for the engineered tissue. The surface properties of the scaffolds are extremely important because they influence the initial cellular events, such as water and ion sorption, protein adsorption and cell adhesion, spreading, and proliferation, in the biomaterial–biological environment. It is not only necessary for the scaffold to be biocompatible and biodegradable; it is also essential that the surface is conducive to cell attachment and subsequent tissue growth.[2]

Cell adhesion is known to be affected by surface roughness and morphology, chemical functionality, electrostatic interaction, surface energy, and biological cues of the surface.[3–5] Surface wettability is an important parameter for cell adhesion on the biomaterial surface because cell adhesion is generally better on hydrophilic surfaces.[6] Therefore, polymer surface modification to improve wettability is of great interest.

Poly(3-hydroxybutyrate-*co*-3-hydroxyvalerate) (PHBV), a natural polyester made by microorganisms via fermentation, has shown great promises as a scaffold biomaterial. PHBV is a biodegradable and biocompatible polymer with a relatively high melting temperature and a crystallinity between 55 and 80%. It is also hydrophobic with an inert surface with a low surface tension and a high contact angle with water.[7,8] The wettability of PHBV has been optimized by blending, chemical modification, plasma treatment, ozone treatment, and gamma radiation in recent years.[9–14] Photografting polymerization was used to obtain polyacrylamide (PAM)-grafted PHBV films in our laboratory. The photografting polymerization of PAM was not only limited to the film surface but

Correspondence to: Y. Wang (imwangyj@scut.edu.cn).
Contract grant sponsor: National Basic Research Program of China; contract grant number: 2005CB623902.
Contract grant sponsor: Guangdong Natural Science Foundation; contract grant number: 4205786.

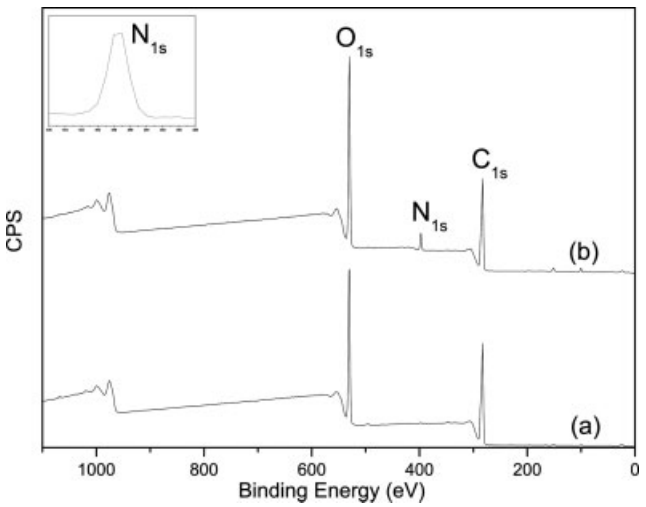

Figure 1 XPS survey spectra of (a) PHBV and (b) PAM-grafted PHBV (CPS-Counts Per Second).

also occurred *in situ* inside the film to form a physical semiinterpenetrating network with a pore microstructure.[15]

In this article, we report the wettability and crystallization behaviors of PAM-grafted PHBV films, with a final aim at wettable surface constructs for tissue engineering applications. Wettability was characterized by water contact angle and water-swelling percentage (WSP) measurements. As discussed later, the wettability of PHBV-*g*-PAM films was influenced by the PAM grafted, PHBV crystallinity, and physical semiinterpenetrating network formed through photografting polymerization. It made it possible for us to obtain desired wettable films by use of the proper PAM grafting percentage (GP). The surface atomic composition and crystallization behaviors were characterized by X-ray photoelectron spectroscopy (XPS), differential scanning calorimetry (DSC), wide-angle X-ray diffraction (WAXD), and polarizing optical microscopy.

EXPERIMENTAL

Materials

PHBV with 8% hydroxyvalerate (HV) content (number-average molecular weight = 1.85×10^5, polydispersity index = 2.2) was purchased from Aldrich Chemical Co., Inc. (Milwaukee, Wisconsin, USA).

We prepared PHBV films by casting the PHBV solution with chloroform as a solvent on a glass plate and drying it at room temperature. The PHBV films obtained were then photografted in aqueous acrylamide under a nitrogen atmosphere. After the reaction, the grafted PHBV films were taken out of the aqueous acrylamide and Soxhlet-extracted with acetone for 48 h. The grafted films were rinsed further with deionized water for 24 h, and the deionized water was replaced three times in the meantime. This purifying treatment is known to basically remove physically attached homopolyacrylamide from grafted films.[15] Four grafted PHBV films with PAM GPs of 6, 17, 53, and 101% were studied.

Characterization

XPS analyses were done on a Kratos (Manchester, England) Axis Ultra^{DCD} X-ray photoelectron spectrometer with a monochromated Al Kα source at a pressure of 2×10^{-9} Torr and a scanning area of 0.7 × 0.3 mm^2. Elemental analysis and quantification spectra from the individual peaks were obtained with a 40-eV pass energy. A value of 285.0 eV for the binding energy of the C_{1s} component was used to correct for the charge of specimens under irradiation. A Gaussian function was assumed for the curve-fitting process.

DSC studies were performed on a Netzsch (Selb, Germany) 204 F1 DSC instrument under a nitrogen atmosphere. The films were heated from −70 to 200°C at a rate of 10°C/min for the first heating run. After they were held at 200°C for 3 min, the films were cooled to −50°C at a rate of −10°C/min for the cooling run. Then, the films were reheated to 200°C at a rate of 10°C/min for the second heating run.

WAXD patterns were recorded from 5 to 70° 2θ in steps of 0.033° on a Philips (Eindhoven, Holland) X'Pert Pro X-ray diffractometer. The applied potential was 40 kV, and the corresponding current was 40 mA. The measuring time was 15.24 s per step.

The crystalline morphology was observed in a Zeiss (Jena, Germany) Axiolab polarizing microscope equipped with a video camera system. The PHBV and grafted PHBV films were initially heated to 200 and 230°C, respectively, at a rate of 50°C/min. After they were held for 3 min, the films were cooled at a rate of 10°C/min to the ambient temperature on a Linkam (Tadworth, England) TH-600 hot stage.

Water contact angles of the films were assessed by a Data Physics OCA 15 (Filder Stadt, Germany) contact angle measurement system at 25°C. The static water-in-air contact angles were calculated as the mean of five replicates. The contact angle data of each sample were the averages of seven individual measurements. Data were expressed as the mean plus or minus the standard deviation of the mean at a significance level of 0.05.

TABLE I
Atomic Percentages of the Films on the Basis of the XPS Survey Spectra

Sample	N_{1s} (atom %)	O_{1s} (atom %)	C_{1s} (atom %)	O/C	N/C
PHBV	0	25.762	74.238	0.35	0
Grafted PHBV	4.276	29.468	66.256	0.45	0.07

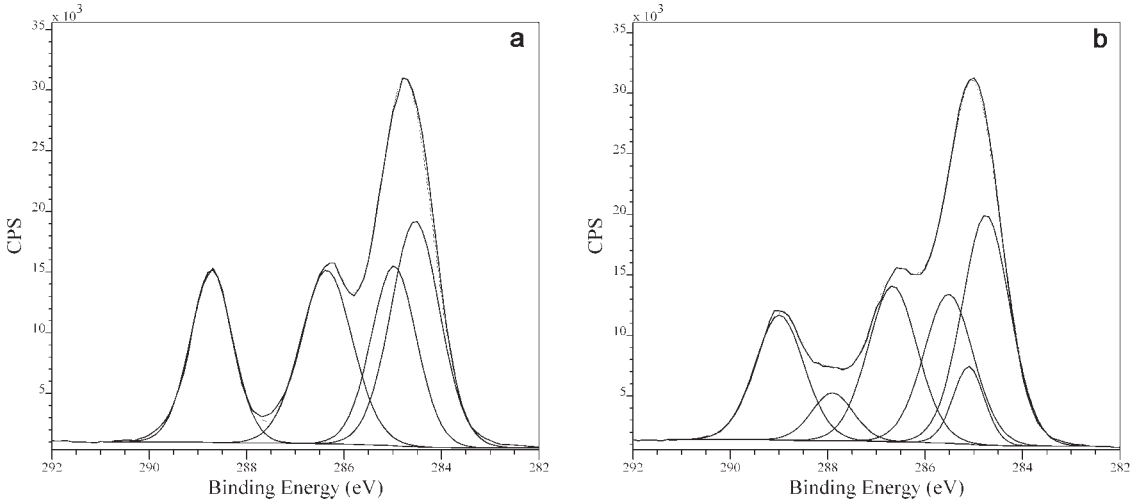

Figure 2 C_{1s} core-level spectra of (a) PHBV and (b) PAM-grafted PHBV. (CPS-Counts Per Second).

WSP was measured by the following method. After they were immersed in water for a given time, the grafted PHBV films with different GPs were blotted quickly with filter paper. WSP was calculated with the following formula:

$$\mathrm{WSP} = (M_1 - M_0)/M_0 \quad (1)$$

where M_0 and M_1 are the masses of the film before and after swelling, respectively. WSP of the grafted PHBV was the average of six replicates.

RESULTS AND DISCUSSION

As mentioned in the preceding article, the structures of the PAM-grafted PHBV films were different according to their GPs.[15] When GP was 6%, PAM chains distributed on the side with irradiation; when GP was 17%, PAM chains appeared not only on the side with irradiation but also inside the PHBV films. However, they did not arrive at the side without irradiation yet. When GP was 53 or 101%, PAM chains appeared on both sides of the PHBV film.

Surface atomic analyses

Atomic compositions of the film surfaces were studied by XPS. Figure 1 presents the survey spectra of the film surfaces, and the corresponding data are summarized in Table I. C_{1s} (binding energy = 285 eV) and O_{1s} (binding energy = 532 eV) peaks appeared in the PHBV. However, an additional N_{1s} peak at 400 eV was noted in the grafted PHBV (17% GP), and the O_{1s} peak became stronger. After photografting polymerization, the carbon composition decreased from 74.24 to 66.25%, whereas the oxygen composition increased from 25.76 to 29.47%. The O/C ratio of PHBV was observed to be 0.35, lower than

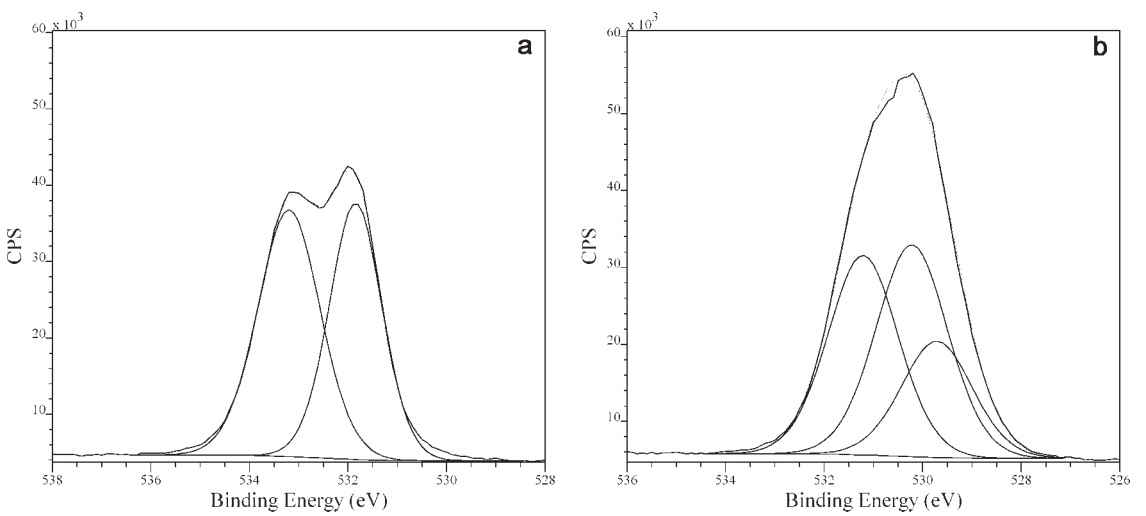

Figure 3 O_{1s} core-level spectra of (a) PHBV and (b) PAM-grafted PHBV. (CPS-Counts Per Second).

TABLE II
Relative Intensities of the Fitted C_{1s} Peaks of the Films

Sample	Position (eV)	Relative intensity (%)	Possible elemental state
PHBV	284.555	31.71	C*—C
	284.947	22.99	C*—C(=O)—O
	286.380	25.16	C*—O
	288.727	20.14	C*(=O)—O
Grafted PHBV	284.808	30.03	C*—C
	285.025	6.60	C*—C(=O)—N
	285.457	19.96	C*—C(=O)—O
	286.660	21.15	C*—O
	287.883	5.99	C*(=O)—N
	288.994	16.27	C*(=O)—O

the expected 1 : 2 on the basis of its repeat units. For the grafted PHBV, the O/C ratio was observed to be 0.45, between 0.33 for PAM and 0.50 for PHBV. Nitrogen from the grafted PHBV film constituted about 4.28 atom % of the total atom. The PHBV film mainly consisted of C and O, which was confirmed by XPS, as shown in Figure 1(a). The N element present on the surface of the grafted PHBV film was attributed to the grafted PAM chains because homopolyacrylamide had been removed basically through Soxhlet extraction with acetone for 48 h and rinsing with deionized water for 24 h after photografting polymerization.

The C_{1s} and O_{1s} core-level spectra, along with the curve fitting, are presented in Figures 2 and 3, respectively. Tables II and III show the relative intensities of the fitted C_{1s} and O_{1s} peaks, respectively. C_{1s} of PHBV had four peaks corresponding to the different chemical bonds of the carbon element: 284.555, 284.947, 286.380, and 288.727 eV, due to C*—C, C*—C(=O)—O, C*—O, and C*(=O)—O, respectively. The relative intensity ratio of 1.6 : 1.1 : 1.2 : 1 was a bit different from the theoretical value (1.1 : 1 : 1 : 1), which suggested the presence of carbon impurities. Two additional peaks at 285.025 and 287.883 eV appeared in C_{1s} of the grafted PHBV with relative intensities of 6.60 and 5.99 atom %, which belonged to C*—C(=O)—N and C*(=O)—N, respectively. As shown in Table II, carbon directly linking to oxygen or nitrogen through single or double bonds was 43.41 atom % for the grafted PHBV film. However, 45.30 atom % of the total carbons were linked to oxygen for the PHBV film. The O_{1s} spectrum of the PHBV could be resolved into two components, the peaks at 531.848 and 533.200 eV, which were attributed to O*=C—O and O*—C, respectively. The relative intensity ratio was close to 1 : 1. These two peaks also presented in the spectrum of the grafted PHBV but at lower binding energies of 530.199 and 531.187 eV. The shifts of the binding energies to lower values were due to the increasing electron density, which was imposed by amide oxygen through steric effects. Apart from these, an oxygen peak with a relative intensity of 45.27 atom % was evident at a slightly lower binding energy of 529.800 eV. It was assigned to O*=C—N for the grafted PHBV. The ratio of amide groups to ester groups on the film surface was calculated to be 1.65 (Table III). On the basis of the C_{1s} and O_{1s} core-level spectra, we concluded that the percentage of the polar functionality on the film surface did not change remarkably; however, only 38 atom % of polar functionality belonged to ester groups after photografting polymerization.

TABLE III
Relative Intensities of the Fitted O_{1s} Peaks of the Films

Sample	Position (eV)	Relative intensity (%)	Possible elemental state
PHBV	531.848	46.75	O*=C—O
	533.200	53.25	O*—C
Grafted PHBV	529.800	45.27	O*=C—N
	530.199	28.26	O*=C—O
	531.187	26.47	O*—C

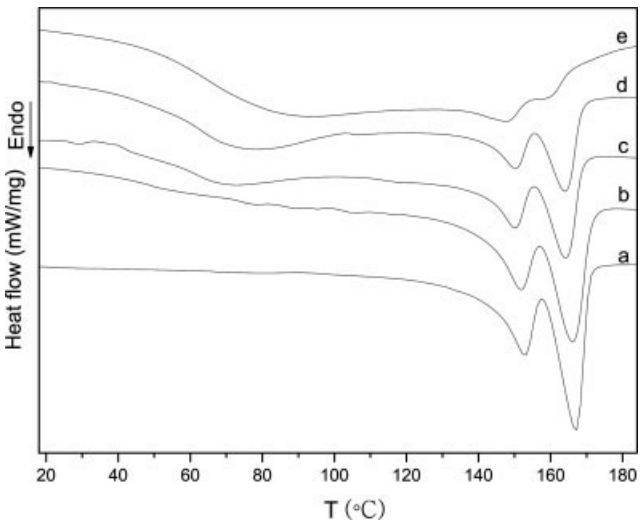

Figure 4 DSC thermograms of (a) PHBV and PAM-grafted PHBV with (b) 6, (c) 17, (d) 53, and (e) 101% GPs (recorded in the first heating run). T = Temperature.

Crystallization behaviors

Crystallization behaviors of the PHBV and grafted PHBV were evaluated by DSC, as shown in Figure 4 and Table IV. Both the PHBV and grafted PHBV exhibited two melting endotherm peaks between 145 and 170°C. The low-temperature endotherm is usually considered to be the true melting behavior of the as-formed crystals, whereas the high-temperature endotherm represents the melting of material that has undergone annealing upon heating.[16] The enthalpy of the low-temperature endotherm peak

TABLE IV
Crystallization Behaviors of PHBV and Grafted PHBV[a]

GP (%)	T_{mL} (°C)	T_{mH} (°C)	ΔH_{fL} (J/g of PHBV)	ΔH_{fH} (J/g of PHBV)	CI (%)
0	152.27	166.27	11.31	25.91	—[b]
6	151.70	166.25	10.40	22.96	89.63
17	150.14	164.33	10.46	18.18	76.95
53	150.30	164.24	7.03	11.77	50.51
101	145.63	157.55	3.05	2.40	14.64

[a] Recorded in the first heating run.
[b] Not detected.

(ΔH_{fL}) and the enthalpy of the high-temperature endotherm peak (ΔH_{fH}) decreased with increasing GP. ΔH_{fH} decreased more quickly, which indicated that the recrystallization of PHBV was suppressed to a large extent after photografting polymerization. To illustrate the change of PHBV's crystallinity after photografting polymerization, a crystallinity index (CI) was defined by the following equation:

$$\mathrm{CI} = (\Delta H_{fL} + \Delta H_{fH})_{\mathrm{grafted}}/(\Delta H_{fL} + \Delta H_{fH})_{\mathrm{PHBV}} \qquad (2)$$

where $(\Delta H_{fL} + \Delta H_{fH})_{\mathrm{grafted}}$ is the total enthalpy per gram of PHBV in the grafted PHBV film and $(\Delta H_{fL} + \Delta H_{fH})_{\mathrm{PHBV}}$ is the total enthalpy per gram of the PHBV film. CI is not the absolute degree of crystallinity, but it could reflects the effect of photografting polymerization on the crystallinity of PHBV. Table IV shows that CI decreased greatly with increasing GP. We believe that the lower crystallinity facilitated the diffusion of water into the film and, thus, enhanced the total water absorption.

The low melting temperature (T_{mL}) and high melting temperature (T_{mH}) of the grafted PHBV were lower than those of PHBV. Both melting temperatures decreased as GP increased. We presumed that grafted PAM was inclined to inducing defects in the interlamellar regions of the PHBV spherulites, and the grafted PHBV with higher GP could induce more defects, which resulted in the lower melting temperatures and enthalpies. As shown in Figure 4, there were special melting endotherm peaks between 60 and 90°C for the grafted PHBV films with 17, 53, and 101% GPs. These melting endotherm peaks were supposed to be the melting of imperfect PHBV crystals formed through photografting polymerization.

WAXD spectra (Fig. 5) were used to understand the crystal structures of PHBV on the PAM-grafted film surfaces. The results show that only a Polyhydroxyrate (PHB) reflection could be found for PHBV because the hydroxybutyrate and HV units cocrystallized within the PHB subcell at HV contents below 30 mol %.[17] There was an increase in *d*-spacing values as a function of GP, especially the (020) and (110) faces, which indicated that the grafted PAM influenced the crystal structure of PHBV.

The model illustrating the transformation of the PHBV crystals is presented in Scheme 1. PHBV possessed spherulite textures [Scheme 1(a)], and the folded polymer chains arranged regularly to form lamellae [Scheme 1(b)]. After photografting polymerization, the grafted PAM chains may wedge into the interlamellar regions of the PHBV spherulites [Scheme 1(c)], tangling *in situ* with the PHBV chains, which perhaps led to the increase in the *d*-spacing value. Once a large amount of the grafted PAM chains were introduced into the interlamellar regions, however, these chains compelled the neighboring lamellar to detach [Scheme 1(d)] or even exfoliate. The endotherm peaks between 60 and 90°C might have been the melting of these imperfect PHBV crystals. Both structures, the crystal structure with increased interplanar crystal spacing and the imperfect crystal structure after partial lamellar detachment or exfoliation, favored the pervasion of small molecules, such as water.

The influence of the grafted PAM on PHBV's recrystallization was also investigated through nonisothermal crystallization and a cold crystallization process and recorded in DSC, as shown in Table V and Figure 6. The melt nonisothermal crystallization

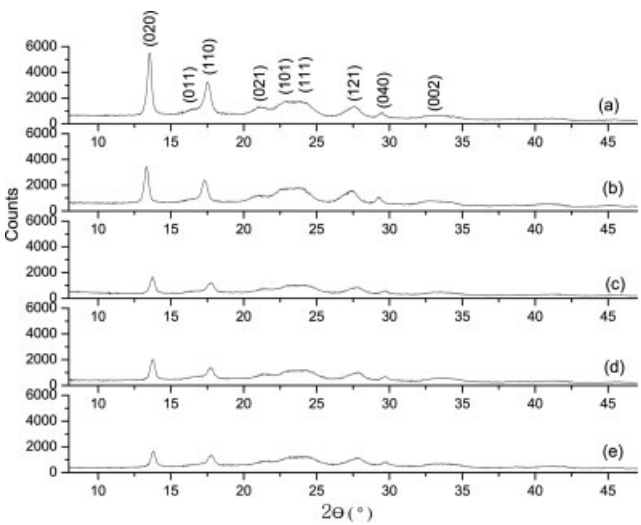

Figure 5 WAXD profiles of (a) PHBV and PAM-grafted PHBV with (b) 6, (c) 17, (d) 53, and (e) 101% GPs.

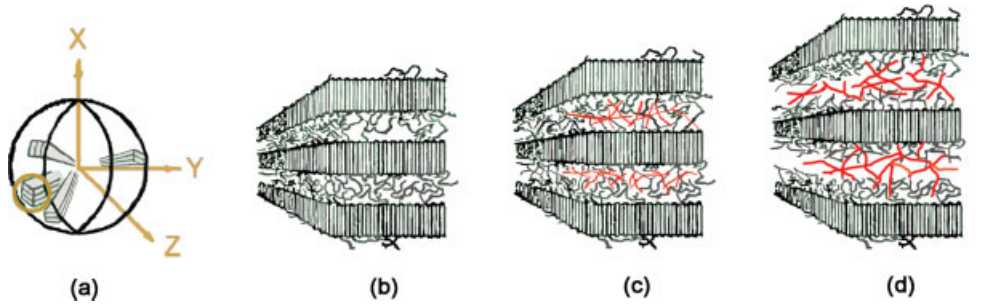

Scheme 1 Model of the PHBV crystal formed after photografting polymerization (the red lines represent grafted PAM chains): (a) PHBV spherulite before the photografting polymerization, (b) PHBV lamella (enlargement in the circle of part a), (c) PHBV lamella with increasing *d*-spacing values after photografting polymerization, and (d) PHBV lamella detached partially after photografting polymerization. [Color figure can be viewed in the online issue, which is available at www.interscience.wiley.com.]

temperature (T_{mc}) decreased, and the cold crystallization temperature (T_{cc}) went up with increasing GP, which suggested the slow crystallization of the grafted PHBV because a lower T_{mc} and a higher T_{cc} indicate slower crystallization.[18] The enthalpies of crystallization decreased with increasing GP. On the basis of the aforementioned results, we concluded that the recrystallization of PHBV after photografting polymerization was suppressed by PAM. To visualize the morphology of crystals formed during the nonisothermal crystallization process, polarizing optical microscopy was conducted. Figure 7 shows the typical PHBV spherulite textures of the films. Spherulites of the PHBV film [Fig. 7(a)] exhibited a Maltese cross birefringence pattern with concentric extinction bands. Figure 7(b,c) shows that the bright spherulites of PHBV dispersed in the dark phases of PAM. Nucleation of PHBV began at about 90.0°C at the edge of the melt, whereas that of the grafted PHBV with 53% GP began at about 51.8°C inside the melt. The maximum diameter of the spherulites formed declined from 350 μm for PHBV to 50 μm for the grafted PHBV with 53% GP. These results reconfirm that the recrystallization of PHBV was hindered by the PAM confinement effect.

TABLE V
Recrystallization Properties of PHBV and Grafted PHBV

GP (%)	T_{mc} (°C)	ΔH_f (J/g of PHBV)[a]	T_{cc} (°C)	$-\Delta H_{cc}$ (J/g of PHBV)[b]
0	60.27	50.25	51.27	3.28
6	59.21	42.77	53.40	5.96
17	59.21	28.28	56.87	12.77
53	55.40	13.25	59.95	19.59
101	—[c]	—[c]	62.28	17.53

[a] Melt nonisothermal crystallization enthalpy.
[b] Cold crystallization enthalpy.
[c] Not detected.

Wettability

PHBV is quite hydrophobic, with its only polar functionality residing in the ester groups, which was confirmed by XPS. It had a significantly high water contact angle (91°), which decreased after photografting polymerization, as shown in Figure 8. A decrease in contact angle was observed with increasing GP. When GP was 53 or 101%, the grafted PHBV films exhibited water contact angles around 60°, which compared well with 56° for PAM acquired under the same circumstances. The amide groups grafted increased the surface polarity. As the surface free energy increased, the water contact angle decreased. The surface wettability improved greatly.

The wettability of the films was also evaluated through WSP, shown in Figure 9. The PHBV film was very hydrophobic and did not absorb water during 6 h of immersion. The grafted PHBV films

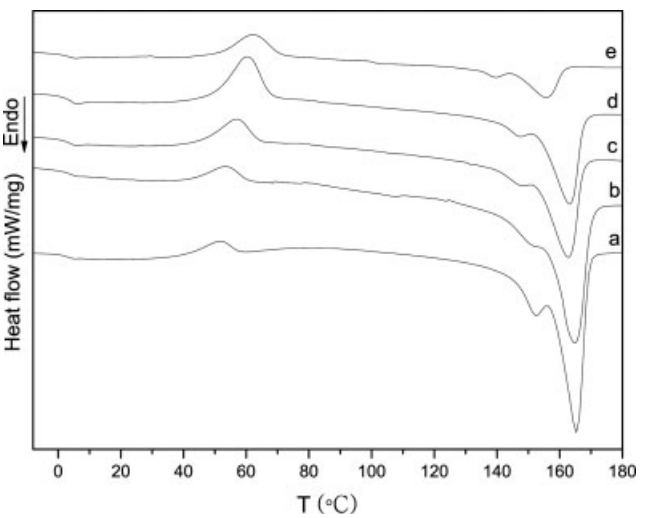

Figure 6 DSC thermograms of (a) PHBV and PAM-grafted PHBV with (b) 6, (c) 17, (d) 53, and (e) 101% GPs (recorded in the second heating run). T = Temperature.

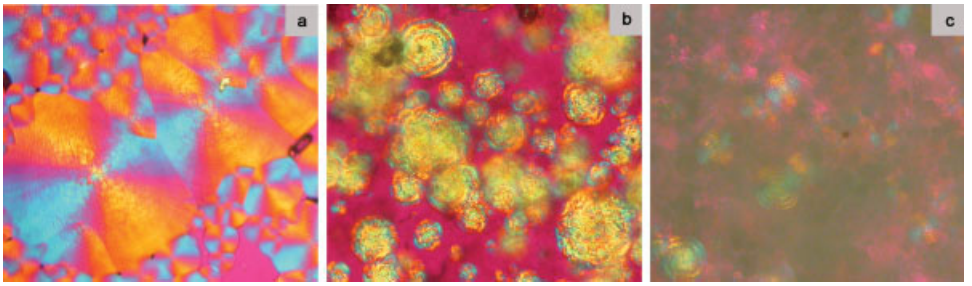

Figure 7 Spherulitic photographs of (a) PHBV and PAM-grafted PHBV with (b) 53 and (c) 101% GPs. [Color figure can be viewed in the online issue, which is available at www.interscience.wiley.com.]

absorbed water rapidly during 5 or 10 min. After that period, WSP increased slightly. As GP increased, WSP went up. The film with 101% GP had the maximum WSP (110%) and swelled uniformly. This phenomenon was attributed to the formation of a semiinterpenetrating network. During photografting polymerization, chains transfer may have occurred and facilitated the crosslinking of the grafted chains to form a semiinterpenetrating network. This network served as a channel to transport water into the grafted PHBV film. Therefore, water absorption occurred not only on the film surface but also inside the film. The semiinterpenetrating network could make it possible for one to obtain a desired wettable inner surface of scaffolds, which may be useful for the improvement of cell adhesion and proliferation for tissue engineering applications.

The good water absorption of the grafted PHBV resulted from the hydrophilic PAM, decreasing crystallinity, and physical semiinterpenetrating network formed through photografting polymerization. When more PAM was grafted or the least crystallinity was obtained, a higher WSP was achieved. In the physical semiinterpenetrating network, there were lots of channels in which water could be held, which led to a further increase in WSP. After photografting polymerization, the wettability of PHBV improved greatly. A hydrophilic film surface with maximum grafting occurring on the surface was obtained by the photografting of PAM with 6 or 17% GP, and the PAM chains grafted decreased from the film surface to the center. However, the grafted PHBV films (53 and 101% GPs) possessed not only the hydrophilic film surface but also the hydrophilic inner surface through the semiinterpenetrating network, although the maximum grafting might not have occurred on the film surface.

CONCLUSIONS

The wettability of PHBV-*g*-PAM films was remarkably improved with increasing PAM GP. The wettability was influenced by PAM, PHBV's crystallinity, and the physical semiinterpenetrating network formed through photografting polymerization. On

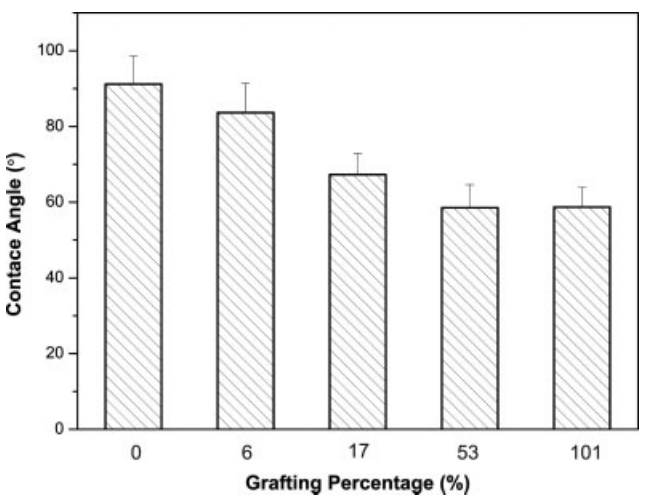

Figure 8 Water contact angle of PHBV and PAM-grafted PHBV with different GPs.

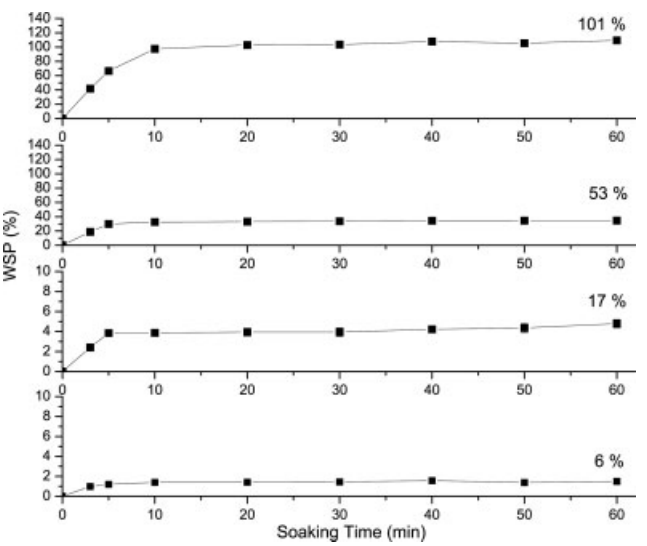

Figure 9 WSP of the PAM-grafted PHBV films with different GPs.

the surface of the grafted PHBV film (17% GP), hydrophilic amide groups were more than hydrophobic ester groups by 24 atom % of total polar functionality. The crystallinity of the films decreased with increasing PAM GP. This was favorable for wettability improvement. The imperfect PHBV crystal structures after photografting polymerization were presumed according to the special melting endotherm peaks between 60 and 90°C and the increase in the *d*-spacing values of the PHBV crystals with PAM GP as well. These imperfect PHBV crystals formed perhaps with increased interplanar crystal spacing or partial lamellar detachment or exfoliation structures could have also facilitated the diffusion of water into the film and, thus, enhanced wettability. In addition, the grafted PAM chains could have also suppressed the recrystallization of PHBV. This study showed a method for improving the wettability of biomaterials for tissue engineering applications by the photografting of hydrophilic monomer on a surface or inside biomaterials to form a physical semiinterpenetrating network. This network brings great promise for wettable surface construction inside tissue engineering scaffolds.

The authors thank associate L. Lu (Southern Medical University, China) for providing helpful suggestions.

References

1. Griffith, L. G.; Naughton, G. Science 2002, 295, 1009.
2. Williams, S. F.; Martin, D. P.; Horowitz, D. M.; Peoples, O. P. Int J Biol Macromol 1999, 25, 111.
3. Fischer, D.; Li, Y. X.; Ahlemeyer, B.; Krieglstein, J.; Kissel, T. Biomaterials 2003, 24, 1121.
4. Boyan, B. D.; Hummert, T. W.; Dean, D. D.; Schwartz, Z. Biomaterials 1996, 17, 137.
5. Ishaug, S. L.; Crane, G. M.; Miller, M. J.; Yasko, A. W.; Yaszemski, M. J.; Mikos, A. G. J Biomed Mater Res 1997, 36, 17.
6. Groth, T.; Altankov, G. Biomaterials 1996, 17, 1227.
7. Chen, G. Q.; Wu, Q. Biomaterials 2005, 26, 6565.
8. Kumarasuriyar, A.; Jackson, R. A.; Grondahl, L.; Trau, M.; Nurcombe, V.; Cool, S. M. Tissue Eng 2005, 11, 1281.
9. Cheng, G. X.; Cai, Z. J.; Wang, L. J Mater Sci: Mater Med 2003, 14, 1073.
10. Saad, B.; Neuenschwander, P.; Uhlschmid, G. K.; Suter, U. W. Int J Biol Macromol 1999, 25, 293.
11. Wang, Y. J.; Lu, L.; Zheng, Y. D.; Chen, X. F. J Biomed Mater Res A 2006, 76, 589.
12. Kose, G. T.; Kenar, H.; Hasirci, N.; Hasirci, V. Biomaterials 2003, 24, 1949.
13. Hu, S. G.; Jou, C. H.; Yang, M. C. J Appl Polym Sci 2003, 88, 2797.
14. Grondahl, L.; Temple, A. C.; Trau, M. Biomacromolecules 2005, 6, 2197.
15. Ke, Y.; Wang, Y. J.; Ren, L.; Lu, L.; Wu, G.; Chen, X. F.; Chen, J. D. J Appl Polym Sci 2007, 104, 4088.
16. Runt, J. P. Macromolecules 1981, 14, 420.
17. Doi, Y.; Kunioka, M.; Nakamura, Y.; Soga, K. Macromolecules 1986, 19, 2860.
18. Kai, W. H.; He, Y.; Inoue, Y. Polym Int 2005, 54, 780.